Development of CdZnTe immersion grating for spaceborne application

Yuki Sarugaku[a], Yuji Ikeda[b,c], Naoto Kobayashi[d], Takashi Sukegawa[e], Shigeru Sugiyama[f], Keigo Enya[a], Hirokazu Kataza[a], Hideo Matsuhara[a], Takao Nakagawa[a], Hideyo Kawakita[c], Sohei Kondo[g], Yasuhiro Hirahara[h], Chikako Yasui[i],

[a]Institute of Space and Astronautical Science, Japan Aerospace Exploration Agency, 3-1-1 Yoshinodai, Chuo-ku, Sagamihara, Kanagawa 252-5210, Japan;
[b]Photocoding, 61-112 Iwakura-KitaIkeda-cho, Sakyo-ku, Kyoto 606-0004, Japan;
[c]Faculty of Science, Kyoto-Sangyo University, Motoyama, Kamigamo, Kita-ku, Kyoto 603-8555, Japan;
[d]Institute of Astronomy, University of Tokyo, 2-21-1 Osawa, Mitaka, Tokyo 181-0015, Japan;
[e]Corporate R&D Headquarters, Canon Inc., 23-10 Kiyohara-Kogyodanchi, Utsunomiya, Tochigi 321-3298, Japan;
[f]Production Engineering Headquarters, Canon Inc., 70-1 Yanagi-cho, Saiwai-ku, Kawasaki, Kanagawa 212-8602, Japan;
[g]Koyama Astronomical Observatory, Kyoto-Sangyo University, Motoyama, Kamigamo, Kita-ku, Kyoto 603-8555, Japan;
[h]Graduate School of Environmental Studies, Nagoya University, Chikusa, Nagoya, Aichi 464-8602, Japan;
[i]Department of Astronomy, University of Tokyo, 7-3-1 Hongo, Bunkyo-ku, Tokyo 113-0033, Japan

ABSTRACT

We have been developing an immersion grating for high-resolution spectroscopy in the mid-infrared (MIR) wavelength region. A MIR (12-18 μm) high-resolution (R = 20,000-30,000) spectrograph with the immersion grating is proposed for SPICA, Japanese next-generation space telescope. The instrument will be the world's first high-resolution spectrograph in space, and it would make great impacts on infrared astronomy. To realize a high-efficiency immersion grating, optical properties and machinability of bulk materials are the critical issues. There are three candidate materials with good MIR transmittance; CdTe (n = 2.65), CdZnTe (n = 2.65), and KRS5 (n = 2.30). From measurements of transmittance with FTIR and of homogeneity with phase-shifting interferometry at 1.55 μm, we confirmed that CdZnTe is the best material that satisfies all the optical requirements. As for machinability, by applying Canon's diamond cutting (planing) technique, fine grooves that meet our requirement were successfully cut on flats for all the materials. We also managed to fabricate a small CdZnTe immersion grating, which shows a high grating efficiency from the air. For the reflective metal coating, we tried Au (with thin underlying layer of Cr) and Al on CdZnTe flats both by sputter deposition and vapor deposition. All samples are found to be robust under 77 K and some of them achieve required reflectivity. Despite several remaining technical issues, the fabrication of CdZnTe immersion grating appears to be sound.

Keywords: immersion grating, SPICA, infrared astronomy, high-resolution spectroscopy, space telescope

Further author information: (Send correspondence to Y.S)
Y.S.: E-mail: sarugaku@ir.isas.jaxa.jp, Telephone: +81 50 336 26286
N.K.: E-mail: naoto@ioa.s.u-tokyo.ac.jp, Telephone: +81 422 34 5032
Y.I.: E-mail: ikeda@photocoding.com, Telephone: +81 75 708 6120

Space Telescopes and Instrumentation 2012: Optical, Infrared, and Millimeter Wave, edited by Mark C. Clampin, Giovanni G. Fazio, Howard A. MacEwen, Jacobus M. Oschmann, Jr., Proc. of SPIE Vol. 8442, 844257

1. INTRODUCTION

1.1 Motivation

High-resolution spectroscopy in the MIR wavelength range is of strong interest. Since numerous rotational-vibration bands of molecules are located in this wavelength range, spectra of celestial objects and ISMs provide fruitful information on physical/chemical condition of them. However, in ground-based observation, systematic observations have been hampered by the strong atmospheric extinction, which limits the observational wavelength range (Fig. 1), and also by the large amount of thermal background, which reduces the sensitivity in most cases. Therefore high-resolution spectroscopy from space has been awaited for investigating the MIR wavelength region, but it has not yet been realized because the size and the weight of instruments for high-resolution spectroscopy are so large and so heavy that it is difficult to launch them. SPICA, which is a next-generation infrared astronomical mission in space with a cooled 3.0 m telescope,[1] is a precious opportunity to explore this exciting field. Mid-infrared Camera and Spectrograph (MCS)[2] is proposed for SPICA. As one function of MCS, we have been developing a high-resolution spectrograph (MCS-HRS).[3] Immersion grating, the main subject of this paper, is the key component for the instrument.

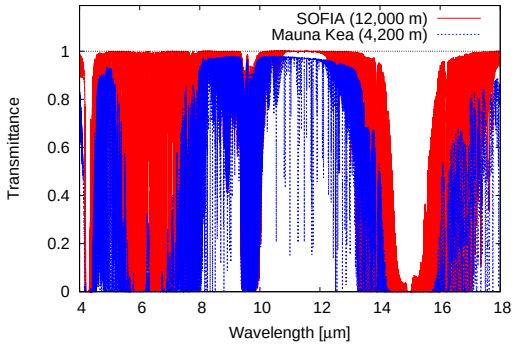

Figure 1. **Atmospheric transmission in the MIR** The transmission was calculated with ATRAN software (Lord 1992, NASA Technical Memorandum 103957). Note even at the SOFIA altitude, strong atmospheric absorption bands still remain at around 15 μm, at which SPICA MCS-HRS will make observations.

The goal of MCS-HRS is to achieve a spectral resolution ($\lambda/\Delta\lambda$) of 20,000-30,000 in the MIR wavelength. In the latest specification, the wavelength coverage is set to be 12-18 μm, where many organic molecules can be detected but it is hard to access from ground due to the strong atmospheric extinction. The main observational targets are ISMs, proto-planetary disks, and comets. The high-resolution capability of the spectrograph enables not only identifying molecular lines but also kinematic studies in the MIR wavelengths. Observing the compositional distribution in proto-planetary disks provides crucial information to understand the formation process of planets. MCS-HRS can shed light on the material evolution among ISMs - proto-planetary disks - comets (planetesimals), and it also has possibility to find molecules some of which could be bio-maker.

We summarize the specification of MCS-HRS in Table 1 and show the optical layout in Fig. 2. It employs transmissive optics to make the spectrograph compact and to relax the fabrication/alignment tolerances. Especially, immersion grating is the key component to achieve high-resolution and high-sensitivity despite of the compact design, which is essential for space instrument. As a result of the conceptual design, diffraction limited resolution is obtained[3] and the sensitivity of this instrument is comparable to that of TMT/MICHI (Table 2). If we focus on observations at wavelengths between 12 μm and 18 μm, MCS-HRS has advantages over MICHI.

1.2 Immersion Grating

Immersion grating is a diffraction grating of which the grooved surface is immersed in a medium with high refractive index (n). It is a powerful optical device for high-resolution spectroscopy. The maximum spectral resolution (R_{max}) of a spectrograph using an immersion grating is given by

$$R_{max} = \frac{\lambda}{\Delta\lambda} = \frac{2n\phi\tan\theta}{\lambda} \quad \text{(in diffraction limited condition)}, \tag{1}$$

Table 1. **Specifications of SPICA MCS-HRS**

Wavelengths	$12 - 18\,\mu$m
Spectral resolution($\lambda/\Delta\lambda$)	20,000 $\sim$ 30,000
Pixel scale	$0.48''$/ pix
Slit length $\times$ width	$6.0'' \times 1.2''$
Main disperser	CdZnTe immersion grating
Detector	Si:As 2048 $\times$ 2048
Size	640mm(L) $\times$ 230mm(W) $\times$ 200mm(H)

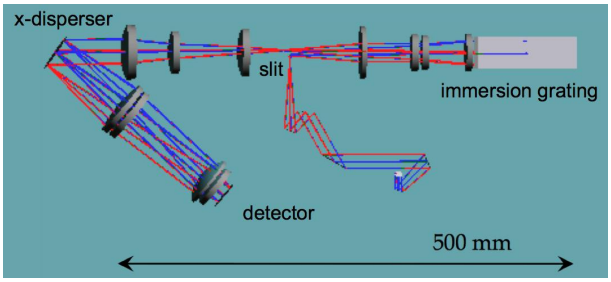

Figure 2. **Optical layout of SPICA MCS-HRS** In addition to the described optics, there is a shared fore-optics to divide light to each function of MCS. The divided light by the fore optics enters to the immersion grating through the collimator lenses. The dispersed light goes through the collimator lenses again, then collimated by the relay optics. This relay optics makes a pupil image on the cross-disperser, resulting in the small size of the entire optical system. The cross-dispersed light enters to the detector through the camera optics.

Table 2. **Comparison of sensitivity**

Telescope/Instrument	Diameter (m)	Waverangth coverage (μm)	Resolving Power	Line Sensitivity at 5σ in 1 hour (10^{-19}W/m^2)		Ref.
				at $\sim$12μm	at $\sim$18μm	
SOFIA/EXES(mid)	2.5	4.5–28.3	1.5×10^4	97	130	[*a*, *b*]
VLT/VISIR	8.2	8–13, 16.5–24.5	$<3\times10^4$	380	670	[*c*, *d*]
GEMINI/Michelle	8.1	7–22	$1–3\times10^4$	34	60	[*e*, *f*]
SPICA/MCS-HRS	3.0	12–18	$2–3\times10^4$	0.3	0.3	
SOFIA/EXES(high)	2.5	4.5–28.3	1×10^5	37	51	[*a*, *b*]
GEMINI/TEXES	8.1	5–25	1×10^5	9	17	[*g*, *h*]
TMT/MICHI(MIRES)	30	8-18 (goal 4.5-28)	1×10^5	0.6	1	[*i*, *j*]

Note.
Since assumptions for sensitivity calculations are not exactly the same, this table has uncertainty in factor level.

Refecences.
[*a*] http://www.physics.ucdavis.edu/exes/
[*b*] http://www.sofia.usra.edu/Science/instruments/instruments_exes.html
[*c*] http://www.eso.org/sci/facilities/paranal/instruments/visir/index.html
[*d*] http://www.eso.org/sci/facilities/paranal/instruments/visir/inst/index.html
[*e*] http://www.gemini.edu/sciops/instruments/michelle/?q=sciops/instruments/michelle
[*f*] http://www.gemini.edu/sciops/instruments/michelle/?q=node/10038
[*g*] http://www.gemini.edu/sciops/instruments/texes/?q=sciops/instruments/texes
[*h*] http://www.gemini.edu/sciops/instruments/texes/sensitivities
[*i*] WWW_MIRES_DRF01.doc in http://www.tmt.org/documents
[*j*] TMT-Instrumentation-and-Performance-Handbook.pdf in http://www.tmt.org/documents

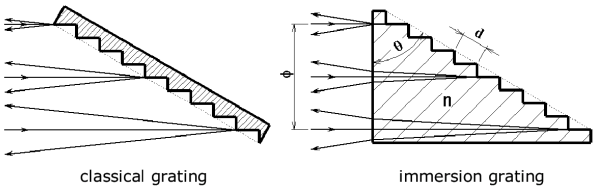

Figure 3. **Classical reflective grating and immersion grating** n: refractive index, ϕ: collimated beam diameter, θ: blaze angle, d: groove pitch.

where ϕ is the collimated beam diameter and θ is the blaze angle (Fig. 3). Eq. 1 demonstrates an immersion grating have n times higher spectral resolution than classical reflective grating of the same size. In other words, a $1/n$-sized immersion grating can provide the same spectral resolution compared to a classical reflective grating, meaning it can reduce the collimated beam and enables compact spectrographs. Therefore, immersion grating is of concern as an optical device to solve the issue of instrument size, which is critical for spaceborne instruments.

The concept of immersion grating was first proposed by Hulthen and Neuhaus in 1954.[4] Although the benefit of immersion grating has been understood for years, it is difficult to develop practical one. In order to realize an immersion grating, we need large optical materials that have high refractive index, low attenuation, and high homogeneity in the wavelength range of interest. The next step is to process grooves with nano-order precision on such materials. Furthermore, the reflective coating on the grating surface and the broadband anti-reflective (BBAR) coating on the entrance/exit surface are necessary to improve the diffraction efficiency. It was in the late 1980s that Dekker[5] proposed the possibility of immersion gratings for astronomical application. In the 1990s, several groups started fabricating Si immersion gratings using anisotropic chemical etching techniques,[6–8] which had been well developed in the semiconductor industry. Marsh et al.[9] finally succeeded in realize a practical Si immersion grating. For observation outside the transmission range of Si (1.2-7.0 μm), studies on Ge immersion gratings, which can cover an atmospheric window in the MIR wavelength range (8-13 μm), had been started.[6,10,11] Since the chemical etching techniques that work well in Si were not applicable to Ge due to the low etch anisotropy, high-precision machining techniques were applied. Ebizuka et al.[10] and Kuzmenko et al.[11] succeeded in ruling grooves on Ge with grinding technique and fly-cutting technique, respectively. Recently, Ikeda et al.[12] have been developing ZnSe immersion grating for short NIR wavelengths (0.9-1.35 μm) with fly-cutting technique. There are several studies on immersion grating but not on that applicable to a wavelength range of 12-18 μm. Therefore, we newly started a development of an immersion gratings for use in the wavelength range.

2. FEASIBILITY STUDY ON MIR IMMERSION GRATING

Even though the downsizing provided by the immersion grating can be a great benefit for space instrument, the first priority issue is the diffraction efficiency of the grating. We aim to achieve a diffraction efficiency comparable to that of reflection grating (goal: >80%, nominal: >60%). The latest design of the immersion grating for SPICA MCS-HRS is shown in Table 3. To achieve high-efficiency, specifications listed in Table 4 are required.

Table 3. **Design of the immersion grating for SPICA MCS-HRS**

Groove pitce	281.23 μm
Blaze angle	75°
Entrance/Exit aperture	30x30 mm

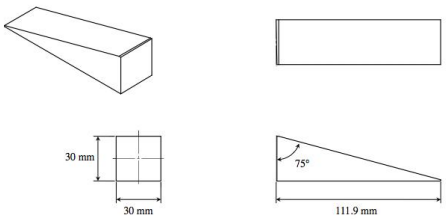

Figure 4. **Drawing of the immersion grating for SPICA MCS-HRS**

Table 4. **Specifications for the immersion grating**

Material	
- Internal attenuation	$\alpha < 0.01$ cm^{-1} @12-18μm
- Homogeneity (in 224-mm path)	$\Delta n < 0.25$ (pv), 0.07 (rms) @12μm
Groove	
- Surface roughness	$H_{rms} < 25$nm (rms)
- Pitch error	$\Delta d < 26$nm (rms)
- Corner R	$C_R < 3.6$ μm
- Surface irregularity	$S < 0.25\lambda$ (pv), 0.07λ (rms) @12μm
Coating	
- Reflectance of the groove surface	$> 95\%$ @12-18μm
- Transmittance of the incident/exit surface	$> 94\%$ @12-18μm

There are three candidates with good MIR transmittance; CdTe ($n = 2.65$), CdZnTe ($n = 2.65$), and KRS5 ($n = 2.30$). Deutsch[13] measured absorption coefficient of a number of potential IR laser window materials and reported the absorption coefficient of CdTe is less than 0.003 cm^{-1} from 2.5 to 20 μm. Hidaka et al.[14] examined transmission loss of some material for MIR optical fibers and reported the absorption coefficient of KRS5 is less than 0.01 cm^{-1} from 10 to 30 μm. Sen et al.[15] investigated the IR transmission behavior of CdZnTe before/after thermal processing to characterize and control the property of CdZnTe substrates for epitaxial growth of HgCdTe. Some CdZnTe samples in their work show $\alpha < 0.05$ cm^{-1} at 12 μm. Although high transmittance of those materials have been demonstrated, commercially available large ingots have the same quality. For example, bulk scattering in polycrystalline materials or carrier density in semiconductor materials can affect the MIR attenuation. Thus, it is necessary to confirm the availability of those large blanks.

To our knowledge, Acrorad (Japan) produces the largest single-crystal CdTe ingot with a diameter of 3-inch (4-inch in experimental stage), JX Nippon Mining & Metals (Japan) produces the largest single-crystal CdZnTe ingot with a diameter of 5-inch (6-inch in experimental stage), and Crystaltechno (Rossia) produces the largest KRS5 blank with a diameter of 200 mm. We purchased samples of those products, and examined attenuation coefficient, homogeneity, and machinability.

2.1 Attenuation Coefficient

The attenuation coefficient α can be derived from transmittance of two substrates with different thickness (t_1 and t_2) as $\alpha = -\ln(T_1 - T_2)/(t_1 - t_2)$, where T_i is the measured transmittance for t_i (i=1, 2).[16] We measured transmittances of the samples with a FTIR (Nicolet Nexus 670 FTIR), however, enough accuracy (< 0.01 cm^{-1}) was not achieved. This is because the samples with the high refractive index elongate optical path length in the FTIR, resulting in that the beam overflows from the detector by defocusing ($t_1 = 3$ mm and $t_2 = 25$ mm in this measurement). The transmittance of thicker sample may be reduced by 10-20%, meaning that α will be overestimated by 0.03-0.08 cm^{-1}. To solve the defocus problem, we are now designing a new optical system correcting the change of the optical path length and pupil position with other FTIR (Jasco FTIR VIR-200).

Despite the problem, the availability of CdZnTe was confirmed. We have CdZnTe samples with different free-carrier densities ($\sim 10^{15}$ cm^{-3} and $\sim 10^{7}$ cm^{-3}), which have different α values. Here, we define α_h and α_l as internal attenuation of samples with high carrier density and that with low carrier density, respectively. The defocus effect can be corrected on the assumption $\alpha_h \gg \alpha_l$ (detail of derivation is in Appendix). This assumption is reasonable in the 8-20 μm range because the attenuation of CdZnTe is proportional to the free-carrier density like CdTe.[15,17] Fig. 5 show the result obtained by this method. The error bars mean the accuracy if the measured transmittances have uncertainties of 1%. Although the estimate is still insufficient, we successfully determined the upper-limit of α_l is $\sim$0.02 cm^{-1}. Furthermore we can assume $\alpha_l \ll 0.01$ cm^{-1} because α_l is expected to be much smaller than α_h,

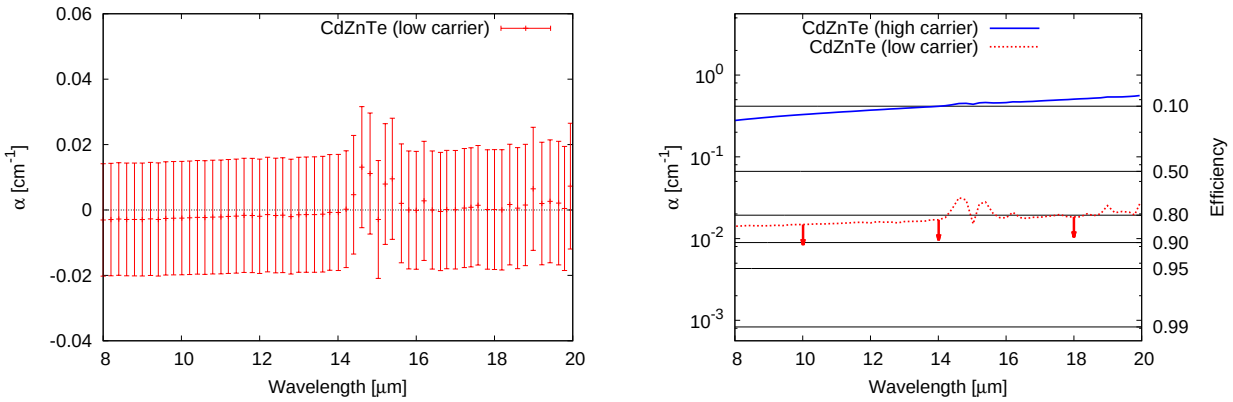

Figure 5. **Attenuation coefficient α of CdZnTe.** (left) α of CdZnTe with low carrier density in linear scale. The absolute values of the calculated α are less than errors which show the accuracy when the measured transmittances have uncertainties of 1%. (right) α of CdZnTe with low and high carrier density in log scale. Here, low and high carrier density shows $\sim 10^7$ cm^{-3} and $\sim 10^{15}$ cm^{-3}.

2.2 Homogeneity

Materials should have good homogeneity (deviation of refractive index n: Δn) so that the wavefront error ($\Delta\lambda$) is less than 0.25λ (pv) and 0.07λ (rms) after the light comes out from an immersion grating. The base length of a immersion grating is 112 mm in the conceptual design. Therefore, Δn is required to be less than 1/4 (pv) and 1/14 (rms) in 224-mm path .

We measured Δn of samples with 3-mm thickness and 20-mm diameter by means of wavelength-shift interferometry. The measured wavelength was 1.55 μm, and measured area was ϕ18 mm. Fig. 6 shows the results (distribution of Δn). The data of KRS5 can not been obtained at this point because of inadequate parallelism of the purchased substrate. The measured Δn is 1.2e-4 (pv) and 8.6e-6 (rms) for CdTe and 6.5e-5 (pv) and 6.3e-6 (rms) for CdZnTe. Supposing the materials have same index distribution everywhere in blanks, we can estimate that Δn of CdTe is 7.6e-4 (pv) and 5.4e-5 (rms) and that of CdZnTe is 4.1e-4 (pv) and 4.0e-5 (rms) in 112-mm thickness (224-mm path), which are much less than the requirement.

Next, we consider a case materials have a deviation of n with larger scale. In Fig. 6, we can see low-frequency components of Δn (scale $\sim$ 6 mm), of which the amplitude is about 3e-5. Since the thickness of sample is 3 mm, the deviation of n due to such large scale can not be included in the measured Δn. Here, we assume that materials have a deviation of n with a typical scale of 6 mm. The pv of Δn in 6-mm scale is estimated to be 3e-5 as the pv of Δn in 3-mm thickness (6-mm path) is 3e-5. If such Δn in 6-mm scale distributes in blanks randomly, the pv of Δn in 224-mm path is calculated to be 2.7e-4, which does not affect the wavefront. Therefore we conclude the homogeneities of CdTe and CdZnTe meet our requirement.

Figure 6. **Homogeneity of CdTe (left) and CdZnTe (right)** Deviation of the refractive index (Δn) in a CdTe and a CdZnTe substrate with a thickness of 3 mm was measured with the wavelength-shift interferometry at 1.55 μm. The aperture size is ϕ18 mm. Obtained Δn of CdTe is 1.2×10^{-4} (pv) and 8.6×10^{-6} (rms). Obtained Δn CdZnTe is 6.5×10^{-5} (pv) and 6.3×10^{-6} (rms).

2.3 Grooves Processing

The appropriate method to process grooves could differ for each material. The classical method for ruling grooves is embossing technique. This technique is useful for ductile materials like metals but not for brittle materials. The chemical etching technique works well for single crystal like Si grating but not for Ge grating because its applicability depends on the etch anisotropy among the direction of the crystal. The alternative process for grooving the brittle materials is machining. A grinding technique at RIKEN[10] and a fly-cutting technique at Lawrence Livermore National Laboratory (LLNL)[11] yielded a good result on processing Ge. Also the fly-cutting technique of LLNL was applied to ZnSe immersion grating,[18] resulting in that grooves with good optical performance are obtained but chippings are seen at the groove facets. To our knowledge, since there are no studies reporting fabrication of immersion grating made of CdTe, CdZnTe, and KRS5 (there are studies on grisms made of KRS5 with ruling technique[19]), we have to establish the feasible process for the materials.

The technique we tried was planing (diamond cutting) using the Free-Form Processing Machine at Canon Inc. (A-Former). In this paper, we show only the result of test cutting on the substrates of the three candidate materials. The Detail of the fabrication procedure is given in Sukegawa et al.[20] Fig. 7 shows the microscope image of the groove facet processed by the A-Former, where the facet had 0.05° slope relative to the substrate plane and the groove pitch was 150 μm. The surfaces looked good with no evidence of chipping, and the surface roughness is < 4 nm in rms, which satisfied our requirement (< 25 nm in rms). Although we had not measured the pitch error of the processed groove, A-Former has good spacing accuracy (< 5nm in rms) which can achieve our requirement (< 26 nm in rms). This accuracy was proved by optical performances of small CdZnTe immersion grating.[20]

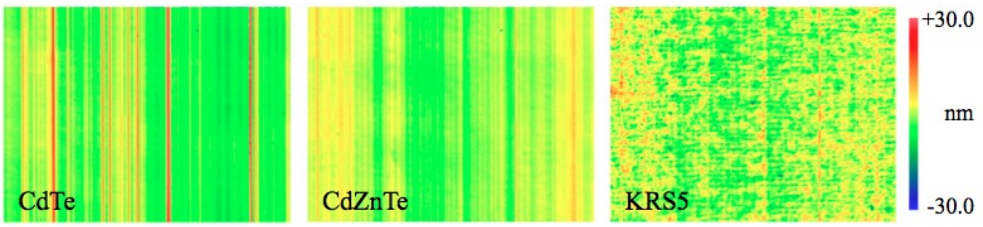

Figure 7. **Microscope images of the groove surface on CdTe, CdZnTe, and KRS5 substrates** The groove was processed by diamond cutting (planing) provided by the Free-Form Processing Machine of Canon (A-Former). The width of images correspond to 140-μm range of a facet (groove pitch is 150 μm). The vertical lines in CdTe are tracks due to chipping of the tool. The measured surface roughnesses (rms) are 3.8 nm (CdTe), 2.9 nm (CdZnTe), and 3.6 nm (KRS5).

2.4 Selection of Material

In table 5 we summarize the result of this feasibility study. Although the evaluation of optical properties is incomplete, we can conclude CdZnTe is the best material because we can get hold of a large ingot with the diameter of 6 inch, which is needed for realizing the immersion grating for MCS-HRS (note: availability of blank depends not only on blank size but also on crystal orientation which restrict cutting direction). Although the ingot with this size is not commercially available at present, we will obtain it with a high possibility because a trial product has already been completed.

Table 5. **Summary of feasibility study**

	Requirement	Single-crystal CdTe	Single-crystal CdZnTe	KRS5
n (@12 μm)	> 2	2.65	$\sim$2.65	2.30
α (@12-18 μm)	< 0.01 cm^{-1}	< 0.003 cm^{-1}(ref.)	< 0.01 cm^{-1}	< 0.01 cm^{-1}(ref.)
Δn in 224-mm path	< 0.25(pv), 0.07(rms)	7.6e-4(pv), 5.4e-5(rms)	4.1e-4(pv), 4.0e-5(rms)	NA
Availability of blank	$>$ 30x30x112 mm	$\times$	$\circ$	$\circ$
Groove	$H_{rms} < 25$nm (rms)	3.8 nm	2.9 nm	3.6 nm
	$\Delta d < 26$nm (rms)	< 4 nm	< 4 nm	< 4 nm

3. FABRICATION OF CDZNTE IMMERSION GRATING

3.1 Small CdZnTe Immersion Grating

We fabricated a CdZnTe immersion grating that has the same groove pitch and blaze angle for MCS-HRS. The entrance/exit aperture is 9.5x9.5 mm. The optical performances of the fabricated grating was measured using the single mode green laser (λ = 543.5 nm). A 2 mm collimated laser beam was irradiated to the diffraction surface from the air space under the Littrow condition. The PSF of the main order (m=1,000) looks slightly asymmetry but is very sharp, which means that it achieves the spectral resolution $\lambda/\Delta\lambda$ = 24,600 whereas the ideal maximum resolution $(\lambda/\Delta\lambda)_{max}$ = 27,500. The diffraction efficiency relative to the ideal grating is >90%. In the immersion grating use at the MIR wavelength, the diffraction efficiency will be much improved because the diffraction orders are much smaller (m $\sim$ 100). See Sukegawa et al.[20] in the detail of the fabrication. In conclusion, a practical immersion grating made of CdZnTe is possible with the current processing technique.

3.2 Reflective Coating for CdZnTe

The Fresnel reflectance of a air-CdZnTe interface is about 20% at λ = 12-18 μm. Hence some kind of coating must be applied to the diffracting surface in order to enhance the absolute efficiency up to the requirement (> 95%). Not only the reflectivity but also the adherability under cryogenic temperature is required for the coating because the immersion grating should be operated at a temperature of 4.5 K.

Metal coatings is a good solution to realize high reflectivity through broadband. Although dielectric coatings also can realize high reflectivity, it often shows high frequent ripples in the spectra which degrade the photometric accuracy. Furthermore, dielectric coatings has following technical issues; (i) There are not many available materials. (ii) Since the coating is composed of many layers, the thickness of each layer must be controlled tightly to obtain the designed performance. (iii) The multilayer results in a thicker coat which induces higher stress to weaken the adhesion of coating.

We consider four common metals with known high reflectivity; Au, Al, Ag, and Cu. Au and Al are well-used and reliable materials for the reflective coating, their reflectivities in the air are higher than 98% at λ = 12-18 μm. In general, the adhesion of Au is so poor that a thin layer of reactive metal is given under Au coating to enhance the adhesion. Cr is a typical metal used as undercoat for Au, but it absorbs IR light. To achieve the reflectivity of 95%, the thickness must be controlled to less than 40 nm. Cr/Au and Al coatings have already been applied not only to metallic mirrors but also to Si or Ge immersion gratings and have demonstrated good performances.[8,9,21] Ag and Cu also have high reflectivity in the MIR wavelengths, but they are reactive metals at room temperature, which require careful handling. Therefore, we selected Cr/Au and Al in the first trial to search useful materials and coating methods for CdZnTe immersion grating.

Since the reflectivity and the adhesion of coating generally depend on the coating method, we experimented different method and temperature condition; (i) sputter deposition at room temperature, (ii) vapor deposition at room temperature, and (iii) vapor deposition with the substrate heated to 200°C. Table 6 summarizes the prepared samples. We measured the reflectivity on CdZnTe-coat boundary (immersed reflectivity) from the CdZnTe side using a FTIR (Jasco FTIR VIR-200). An Al mirror was used as the reference, and the angle of incident light is 12° from the normal direction of the sample surface. As the obtained raw data include the

Table 6. **Relective coating samples** Prior to the vapor deposition, the surface of substrates were activated by Ar ion sputtering.

No.	Material	Thickness	Method	Substrate temperature
1	Al	300 nm	sputter deposition	room temp.
2	Al	300 nm	vapor deposition	room temp.
3	Al	300 nm	vapor deposition	200°C
4	Cr/Au	2 nm / 300 nm	sputter deposition	room temp.
5	Cr/Au	2 nm / 300 nm	vapor deposition	room temp.
6	Cr/Au	2 nm / 300 nm	vapor deposition	200°C

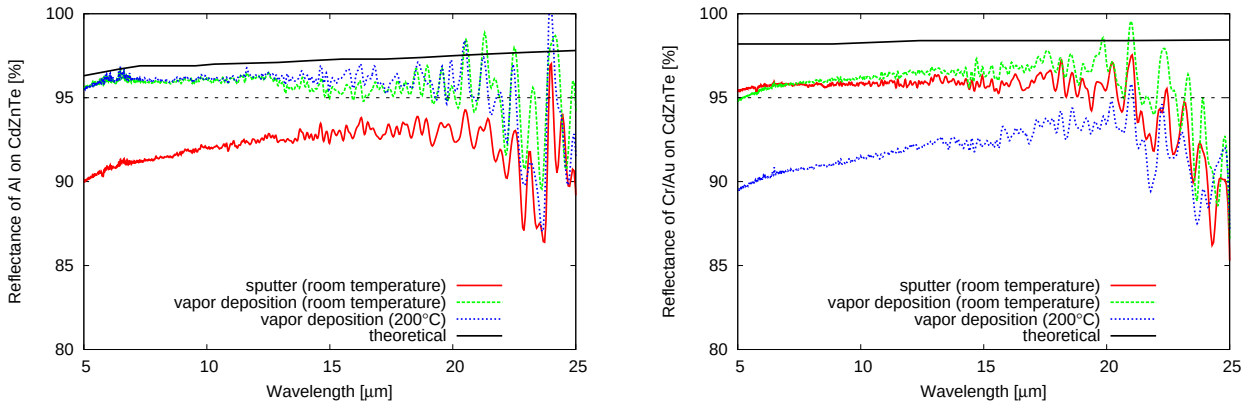

Figure 8. **Immersed reflectivity on CdZnTe-Al (left) and CdZnTe-Cr/Au (right) boundary**

light reflected on the air-CdZnTe interface, we corrected the immersed reflectivity by assuming (i) the measured reflectivity contains all light multiple-reflected within the substrate, (ii) no energy is absorbed by the CdZnTe substrate, and (iii) the refractive index of CdZnTe is same as that of CdTe. The results are shown in Fig. 8. We can see No. 2, 3, 4, and 5 achieve the required reflectivity. The cause of the difference in reflectivity among samples is under discussion.

In order to evaluate the coating durability under cryogenic temperature, we cooled the samples by dipping them into liquid nitrogen. After the cryogenic testing, no alternation was observed to the eye. Also the change in reflectivity was within the measurement error.

4. SUMMARY AND FUTURE WORK

We started a study on immersion grating for high-resolution spectroscopy in the mid-infrared wavelength region. First, we examined the optical properties of three candidate materials with good MIR transmittance; CdTe, CdZnTe, and KRS5. From measurements of transmittance with FTIR, the upper-limit of the attenuation coefficient was successfully obtained for CdZnTe ($\alpha < 0.02$ cm^{-1}). Considering the dependence of α on free-carrier density, we can assume CdZnTe satisfies our requirement ($\alpha < 0.01$ cm^{-1}). Also, we confirmed that CdZnTe meet the requirement for homogeneity ($\Delta n < 0.25$ in pv and 0.75 in rms for 224-mm path) with phase-shifting interferometry at 1.55 μm. Next, we examined the machinability of the materials by applying Canon's diamond cutting (planing) technique. As a result, fine grooves that meet our requirement (surface roughness < 25 nm in rms, pitch error < 26 nm in rms, and corner R < 3.6 μm) were successfully cut on flats for all the materials. Since only CdZnTe is available in large blanks with good optical quality at this point, we have chosen CdZnTe as the first candidate. Finally, we managed to fabricate a small CdZnTe immersion grating[20] that has the same groove pitch and blaze angle designed for MCS-HRS. Optical performances measured from the air space proved the possibility of manufacturing a practical immersion grating. To search useful materials and coating methods for reflecting coating, we put Cr/Au and Al on CdZnTe flats both by sputter and vapor deposition. As a result, we obtained sufficient reflectivity for some of them and confirmed the coating durability at 77 K for all of them.

Although we concluded the transparency of CdZnTe is satisfactory, the measurement accuracy is insufficient to determine their absolute attenuation coefficients. We are now designing an optical system to improve the measurement accuracy of the FTIR. Since the immersion grating should be operated at 4.5 K, we have to conduct cryogenic testing of the coating durability at the temperature. After the reflective coating on the flat surface is established, test coatings on the grooved surface have to be carried out. In addition to the reflective coating, BBAR coating on the entrance/exit surface remains as the final technical issue to realize a useful immersion grating.

APPENDIX A. ATTENUATION COEFFICIENT OF CDZNTE

We show the derivation of the attenuation coefficient of CdZnTe using transmittances measured with FTIR. The parameters of samples we used are shown in Table 7. We define α_h as internal attenuation of samples with high carrier density and α_l as that with low carrier density. Also we describe measured transmittances as T_{ij} for samples with a internal attenuation of α_i and a thickness of t_j ($i = h$, l and $j = 1$, 2). If we assume multiple-reflection within the substrate, T_{ij} are given by,

$$T_{h1} = \frac{k_1(1-R_s)^2\exp(-\alpha_h t_1)}{1-R_s^2\exp(-2\alpha_h t_1)}, \tag{2}$$

$$T_{h2} = \frac{k_2(1-R_s)^2\exp(-\alpha_h t_2)}{1-R_s^2\exp(-2\alpha_h t_2)}, \tag{3}$$

$$T_{l1} = \frac{k_1(1-R_s)^2\exp(-\alpha_l t_1)}{1-R_s^2\exp(-2\alpha_l t_1)}, \tag{4}$$

$$T_{l2} = \frac{k_2(1-R_s)^2\exp(-\alpha_l t_2)}{1-R_s^2\exp(-2\alpha_l t_2)}, \tag{5}$$

where R_s is the surface reflection and k_1 and k_2 are factors to express the decrease of signals due to the defocus effect. From Eq. 3 and Eq. 5, we have

$$\alpha_h = -\frac{\ln(\frac{T_{h2}}{T_{l2}})}{t_2} \tag{6}$$

by assuming

$$\frac{1-R_s^2\exp(-2\alpha_h t_2)}{1-R_s^2\exp(-2\alpha_l t_2)} \sim 1 \quad \text{and} \quad \alpha_h \gg \alpha_l. \tag{7}$$

Then, dividing Eq. 2 by Eq. 3 with substitution of α_h leads to the k_1/k_2 ratio. Finally, dividing Eq. 4 by Eq. 5, we obtain α_l by

$$\alpha_l = -\frac{\ln(\frac{T_{l1}k_2}{T_{l2}k_1})}{t_1 - t_2} \tag{8}$$

on the assumpion that

$$\frac{1-R_s^2\exp(-2\alpha_l t_1)}{1-R_s^2\exp(-2\alpha_l t_2)} \sim 1 \tag{9}$$

Table 7. **Parameter of samples**

suffix	free-carrier density (cm^{-3})	thickness (mm)
$h1$	$\sim 10^{15}$	3
$h2$	$\sim 10^{15}$	3
$l1$	$\sim 10^{7}$	25
$l2$	$\sim 10^{7}$	25

ACKNOWLEDGMENTS

We thank Dr. Ryuichi Hirano (JX Nippon Mining & Metals) for useful comment on material properties. We also thank Prof. Chiyoe Koike and Dr. Hiroki Chihara (Osaka Univ.) for supporting measurement with FTIR. This work is financially supported by the MEXT- Supported Program for the Strategic Research Foundation at Private Universities (2008-2012). This study is also financially supported by KAKENHI (24740131) Grant-in-Aid for Young Scientists (B) by Japan Society for the Promotion of Science.

REFERENCES

[1] Nakagawa, T., Matsuhara, H., and Kawakatsu, Y., "The next-generation infrared space telescope SPICA," *Proc. SPIE* **8442** (July 2012).

[2] Kataza, H., Wada, T., Sakon, I., Kobayashi, N., Sarugaku, Y., Ikeda, Y., Fujishiro, N., and Oyabu, S., "Mid-infrared camera and spectrometer on board SPICA," *Proc. SPIE* **8442** (July 2012).

[3] Kobayashi, N., Ikeda, Y., Kawakita, H., Enya, K., Nakagawa, T., Kataza, H., Matsuhara, H., Hirahara, Y., and Tokoro, H., "Mid-infrared high-resolution spectrograph for SPICA," *Proc. SPIE* **7010**, 701032 (Aug. 2008).

[4] Hulthén, E. and Heuhaus, H., "Diffraction Gratings in Immersion," *Nature* **173**, 442–443 (Mar. 1954).

[5] Dekker, H., "An Immersion Grating for an Astronomical Spectrograph," *The Ninth Santa Cruz Summer Workshop in Astronomy and Astrophysics*, 183–188 (1988).

[6] Wiedemann, G. and Jennings, D. E., "Immersion grating for infrared astronomy," *Applied Optics* **32**, 1176–1178 (Mar. 1993).

[7] Graf, U. U., Jaffe, D. T., Kim, E. J., Lacy, J. H., Ling, H., Moore, J. T., and Rebeiz, G., "Fabrication and evaluation of an etched infrared diffraction grating," *Applied Optics* **33**, 96–102 (Jan. 1994).

[8] Kuzmenko, P. J., Ciarlo, D. R., and Stevens, C. G., "Fabrication and testing of a silicon immersion grating for infrared spectroscopy," *Proc. SPIE* **2266**, 566–577 (Sept. 1994).

[9] Marsh, J. P., Mar, D. J., and Jaffe, D. T., "Production and evaluation of silicon immersion gratings for infrared astronomy," *Applied Optics* **46**, 3400–3416 (June 2007).

[10] Ebizuka, N., Morita, S., Shimizu, T., Yamagata, Y., Omori, H., Wakaki, M., Kobayashi, H., Tokoro, H., and Hirahara, Y., "Development of immersion grating for mid-infrared high dispersion spectrograph for the 8.2m Subaru Telescope," *Proc. SPIE* **4842**, 293–300 (Feb. 2003).

[11] Kuzmenko, P. J., Davis, P. J., Little, S. L., Little, L. M., and Bixler, J. V., "High efficiency germanium immersion gratings," *Proc. SPIE* **6273**, 62733T (July 2006).

[12] Ikeda, Y., Kobayashi, N., Kuzmenko, J. P., Little, S. L., Yasui, C., Kondo, S., Mito, H., Nakanishi, K., and Sarugaku, Y., "Fabrication and current optical performance of a large diamond-machined ZnSe immersion grating," *Proc. SPIE* **7739**, 77394G (July 2010).

[13] Deutsch, T. F., "Absorption coefficient of infrared laser window materials*," *Journal of Physics and Chemistry of Solids* **34**, 2091–2104 (Dec. 1973).

[14] Hidaka, T., Morikawa, T., and Shimada, J., "Spectroscopic small loss measurements on infrared transparent materials," *Applied Optics* **19**, 3763–3766 (Nov. 1980).

[15] Sen, S., Rhiger, D. R., Curtis, C. R., Kalisher, M. H., Hettich, H. L., and Currie, M. C., "Infrared absorption behavior in CdZnTe substrates," *Journal of Electronic Materials* **30**, 611–618 (June 2001).

[16] Ikeda, Y., Kobayashi, N., Kondo, S., Yasui, C., Kuzmenko, P. J., Tokoro, H., and Terada, H., "Zinc sulfide and zinc selenide immersion gratings for astronomical high-resolution spectroscopy: evaluation of internal attenuation of bulk materials in the short near-infrared region," *Optical Engineering* **48**, 084001 (Aug. 2009).

[17] Jensen, B., "Free carrier absorption in n-type CdTe," *Journal of Physics and Chemistry of Solids* **34**, 2235–2245 (Dec. 1973).

[18] Ikeda, Y., Kobayashi, N., Kondo, S., Yasui, C., Motohara, K., and Minami, A., "WINERED: a warm near-infrared high-resolution spectrograph," *Proc. SPIE* **6269**, 62693T (July 2006).

[19] Weitzel, L., Krabbe, A., Kroker, H., Thatte, N., Tacconi-Garman, L. E., Cameron, M., and Genzel, R., "3D: The next generation near-infrared imaging spectrometer," *Astronomy and Astrophysics Supplement* **119**, 531–546 (Nov. 1996).

[20] Sukegawa, T., Sugiyama, S., Kitamura, T., Okura, Y., and Koyama, M., "High-performance astronomical gratings by Canon," *Proc. SPIE* **8450** (July 2012).

[21] Kuzmenko, P. J., Little, L. M., Davis, P. J., and Little, S. L., "Modeling, fabrication, and testing of a diamond-machined germanium immersion grating," *Proc. SPIE* **4850**, 1179–1190 (Mar. 2003).